# A Microstructural Approach to Cytoskeletal Mechanics based on Tensegrity

DIMITRIJE STAMENOVIĆ†, JEFFREY J. FREDBERG‡, NING WANG‡, JAMES P. BUTLER‡ AND DONALD E. INGBER§

† *Department of Biomedical Engineering, Boston University, Boston, MA* 02215, ‡ *Physiology Program, Department of Environmental Health, Harvard School of Public Health and* § *Departments of Surgery and Pathology, Children's Hospital and Harvard Medical School, Boston, MA* 02115, *U.S.A.*

Mechanical properties of living cells are commonly described in terms of the laws of continuum mechanics. The purpose of this report is to consider the implications of an alternative approach that emphasizes the discrete nature of stress bearing elements in the cell and is based on the known structural properties of the cytoskeleton. We have noted previously that tensegrity architecture seems to capture essential qualitative features of cytoskeletal shape distortion in adherent cells (Ingber, 1993a; Wang *et al.*, 1993). Here we extend those qualitative notions into a formal microstructural analysis. On the basis of that analysis we attempt to identify unifying principles that might underlie the shape stability of the cytoskeleton. For simplicity, we focus on a tensegrity structure containing six rigid struts interconnected by 24 linearly elastic cables. Cables carry initial tension ("prestress") counterbalanced by compression of struts. Two cases of interconnectedness between cables and struts are considered: one where they are connected by pin-joints, and the other where the cables run through frictionless loops at the junctions. At the molecular level, the pinned structure may represent the case in which different cytoskeletal filaments are cross-linked whereas the looped structure represents the case where they are free to slip past one another. The system is then subjected to uniaxial stretching. Using the principal of virtual work, stretching force vs. extension and structural stiffness vs. stretching force relationships are calculated for different prestresses. The stiffness is found to increase with increasing prestress and, at a given prestress, to increase approximately linearly with increasing stretching force. This behavior is consistent with observations in living endothelial cells exposed to shear stresses (Wang & Ingber, 1994). At a given prestress, the pinned structure is found to be stiffer than the looped one, a result consistent with data on mechanical behavior of isolated, cross-linked and uncross-linked actin networks (Wachsstock *et al.*, 1993). On the basis of our analysis we concluded that architecture and the prestress of the cytoskeleton might be key features that underlie a cell's ability to regulate its shape.

© 1996 Academic Press Limited

## Introduction

Mechanical stresses on cells, such as those imposed by hemodynamic forces, gravity or cell-generated tension, are known to regulate tissue growth and development and to alter cell form and function (Ingber, 1991; Davis & Tripathi, 1993). For example, when adherent endothelial cells are exposed to flow-induced shear stresses, the cytoskeleton (CSK) undergoes major structural reorganization, the topological profile of cell height changes, ion channels become activated, acetylcholine and substance P are released, and changes in gene expression occur (Davis & Tripathi, 1993). Since many elements of the cell's metabolic machinery appear to be immobilized on insoluble support scaffolds, changes in cell function may result from CSK remodeling and structural rearrangement (Ingber, 1993b). As such, the mechanical basis of CSK deformability becomes of central interest.

† Author to whom correspondence should be addressed. E-mail: dimitrije@enga.bu.edu

The standard approach in cell mechanics is based upon the continuum hypothesis. It views the cell as a continuous elastic cortical shell surrounding a continuous viscous or viscoelastic core (*cf*. Elson, 1988; Evans & Yeung, 1989; Fung & Liu, 1993). Shape distortion of the cell is assumed to result primarily from stresses distributed over the cell membrane and transmitted throughout the cytoplasm following the laws of continuum mechanics. This view of CSK deformability has been fruitful. The continuum hypothesis rests on the premise that a scale which is small compared with the cell, but large compared with the distance between microstructural elements, the microstructure itself need not be taken into account explicitly. The physical attributes (mass, force, stiffness, strain energy, friction) and deformation within a given small volume are assumed to be spread continuously throughout that volume rather than being concentrated in a small fraction of it.

The purpose of this report is to consider the implications of an alternative viewpoint that emphasizes the discrete nature of stress bearing elements in the cell and is based on known properties of the CSK. Our rationale is as follows. In contrast to the continuum perspective, it is now firmly established that force transmission between the cell and the extracellular milieu occurs at focal adhesion sites and is mediated by specific trans-membrane receptors, such as integrins, that form discrete molecular bridges that interlink intracellular CSK filaments with extracellular matrix anchoring scaffolds (Ingber, 1991; Schiro *et al*., 1992; Schmidt *et al*., 1993; Wang *et al*., 1993; Scott-Burden, 1994). It is also well established on structural grounds that the CSK is an interconnected lattice comprised of discrete microfilaments, microtubules, and intermediate filaments (*cf*. Amos & Amos, 1991; Ingber, 1993a). Although much is known about the molecular constituents of the adhesion complexes and the CSK matrix, there is little understanding of how these components are organized architecturally or how they act to resist shape distortion. To our knowledge, no attention has been focused on the issue of the degree to which deformation of this lattice might conform to the tenets of the continuum hypothesis or on the implications of departures therefrom.

We have previously noted that eukaryotic cells display both CSK structure and elastic deformability that appear to be consistent with so-called tensegrity (tensional integrity) architecture as first described by Buckminster Fuller (Fuller, 1961; Ingber & Jamieson, 1985; Ingber, 1993a; Wang *et al*., 1993; Ingber *et al*., 1994). In its simplest representation, Pugh (1976) defined tensegrity structures as the interaction of a set of discontinuous (isolated) compression elements (e.g., struts) with a set of continuous tension elements (e.g., cables) in the aim to provide a stable volume and shape in the space. The tension elements carry "prestress" (i.e., initial stress), conferring load-supporting capability to the entire structure. The role of the compression elements is to provide prestress in the tension elements. Together, they form a self-equilibrating, stable mechanical system.

A distinguishing characteristic of the tensegrity structure is that in order to express a resistance to distortion of shape it requires a prestress in its members even before the external load is applied. Examples of tensegrity structures in nature include spider webs, gas-liquid foams, plant leaves, and mammalian lungs. In the case of foams, leaves, and lungs the prestress is provided by the pressure of the inflating fluid (the compression element in lieu of rigid struts), and is carried by lattice tension elements (e.g., liquid films in foams). In the case of spider webs, the prestress is provided by discrete attachments to surrounding objects, such as tree branches, and is balanced by tension in web threads. Even though they are external to the web itself, the tree branches may be viewed as the compression elements in a tensegrity structure, because they are an integral part of the mechanically stable whole. In the absence of the prestress, the intrinsic resistance to shape distortion is lacking in these structures because their internal degrees of freedom of motion are not fully constrained. In the presence of a prestress, however, the structural elements move relative to one another until they attain a configuration which provides equilibrium between external shear forces and those carried by the structural elements. The larger the initial forces carried by those elements (i.e., the larger the prestress), the smaller the deformation those structures would undergo at a given shear stress before they attain a new equilibrium configuration.

A key feature of any tensegrity structure is the interconnectedness of its elements, i.e., the manner in which structural elements are mutually connected and the degree of relative motion between interconnecting elements at their junctions. For example, interconnection between liquid films in foams is such that at equilibrium surface forces carried by those films are equal. This type of interconnectedness yields minimal shear stiffness (Stamenović, 1991).

It is likely that the CSK together with the extracellular matrix form a tensegrity structure (Ingber, 1993a; Ingber *et al*., 1994). For example, the regions of extracellular matrix that stretch between focal contacts represent local compression-resistant elements which resist the tension exerted by

stress-fibers inside the cell (Harris *et al*., 1980; Ingber, 1993a). Within the CSK of living cells, microtubule bundles act as compression-resistant struts and stabilize cell shape by resisting the pull of the contractile actin lattice (Joshi *et al*., 1985; Dennerll *et al*., 1988; Danowski, 1989; Kolodney & Wysolmerski, 1992; Heidemann & Buxbaum, 1994).

Model structures built of sticks and elastic strings according to the rules of tensegrity architecture qualitatively mimic many of the phenomena that have been observed in living cells including the effects of substrate adhesion on cell shape, cell polarity, and CSK remodeling (Ingber & Jamieson, 1985; Ingber, 1993a; Ingber *et al*., 1994). These tensegrity structures also exhibit a nearly linear dependence between the stiffness of the entire structure and the applied stress, over a wide range of stresses (Wang *et al*., 1993). Importantly, this peculiar "linear stiffening" response appears to be a fundamental property of living cells (Wang *et al*., 1993; Wang & Ingber, 1994) as well as tissues (*cf*. Fung, 1981). While the characteristic linear stiffening can be predicted by empirical relationships (Mow *et al*., 1992) or phenomenological models (Frisén *et al*., 1969), these approaches have not been able to explain the observed phenomena based on first principles (McMahon, 1984).

In the sections below we extend these qualitative notions into a formal microstructural analysis. On the basis of that analysis we attempt to identify unifying principles that might underlie shape stability of the CSK. For simplicity, we focus on a tensegrity structure containing six rigid struts interconnected by 24 linearly elastic cables; such a simple tensegrity structure embodies the same essential features observed in structures with different arrangements and numbers of structural elements as well as in hierarchical arrangements of different sized tensegrity arrays. Most importantly, we do not view this six-strut structure as a direct, one-to-one model of some part of the CSK. Rather, it is a plausible description of the mechanisms that regulate cell shape stability for which a quantitative basis has been lacking in the past. The six-strut tensegrity structure was subjected to uniaxial stretching and corresponding force vs. extension relationships were calculated for different prestresses and for different types of interconnectedness of structural elements, starting from first principles of mechanics. This approach elucidates how simple tensegrity structures naturally come to express many of the seemingly complex behaviors observed in living cells exposed to shearing forces. This does not at all preclude the numerous chemically mediated mechanisms which are known to regulate CSK filament assembly. Rather, it elucidates

a higher level of organization in which biochemical remodeling events function and also may be regulated.

## Method

### DESCRIPTION OF THE PROTOTYPE TENSEGRITY STRUCTURE

The CSK is assumed to be organized as a tensegrity structure (Ingber & Jamieson, 1985; Ingber *et al*., 1994). Thus, to simplify our approach, a six-strut tensegrity structure (Fig. 1) was considered as a first step in implementing tensegrity architecture in studies of cell mechanics.

The six-strut tensegrity structure is composed of 24 cable segments and six struts. In this study, the cables are viewed as elastic elements which support only tension forces whereas the struts are viewed as rigid bars under compression. The struts are slender and support no lateral load. At the reference (initial) state, compression forces in the struts balance tension forces in the cables. The initial tension is referred to as a prestress. Within the CSK, microfilaments and intermediate filaments may play the role of cables
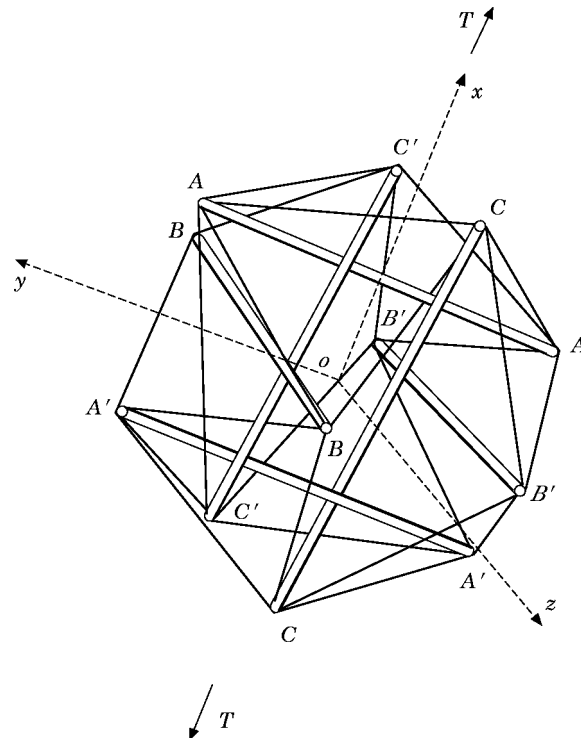


FIG. 1. Six-strut tensegrity model. Struts: $\overline{AA}$, $\overline{A'A'}$, $\overline{BB}$, $\overline{B'B'}$, $\overline{CC}$, $\overline{C'C'}$; cables: $\overline{AB}$, $\overline{AC}$, $\overline{BC}$, $\overline{A'B}$, $\overline{A'C}$, $\overline{B'C}$, $\overline{AB'}$, $\overline{AC'}$, $\overline{BC'}$, $\overline{A'B'}$, $\overline{A'C'}$, $\overline{B'C'}$. Pulling forces of magnitude $T/2$ (not shown) are applied at each end of struts $\overline{AA}$ and $\overline{A'A'}$, along the $Ox$-axis. The resultant stretching force $T$ is indicated by the thick arrows.

whereas microtubules or cross-linked actin bundles may play the role of struts (Ingber, 1993a).

The origin $O$ of a rectangular Cartesian coordinate system $Oxyz$ is placed at the center of the structure, with the $Ox$-axis parallel to the struts $\overline{CC}$ and $\overline{C'C'}$, $Oy$-axis parallel to the struts $\overline{AA}$ and $\overline{A'A'}$, $Oz$-axis parallel to the struts $\overline{BB}$ and $\overline{B'B'}$ (Fig. 1).

<center>GEOMETRIC CONSIDERATIONS</center>

For convenience, the struts are assumed to be of unit length. Thus, at the reference state the length of each cable segment is $l_0 = \sqrt{0.375}$ and the distance between parallel struts $s_0 = 0.5$ (Kenner, 1976).

The structure is stretched in the direction of the $Ox$-axis (axial direction) by pulling the struts $\overline{AA}$ and $\overline{A'A'}$ apart by forces of magnitude $T/2$ applied at each endpoint of these two struts. The resultant pulling (stretching) force is, therefore, $T$ (Fig. 1). This causes changes in the distances between the pairs of parallel struts from $s_0$ to: $s_x$ for the struts $\overline{AA}$ and $\overline{A'A'}$, $s_y$ for the struts $\overline{BB}$ and $\overline{B'B'}$, and $s_z$ for the struts $\overline{CC}$ and $\overline{C'C'}$, and changes in the cable lengths from $l_0$ to: $l_1 = \overline{AB} = \overline{A'B} = \overline{AB'} = \overline{A'B'}$, $l_2 = \overline{BC} = \overline{B'C} = \overline{BC'} = \overline{B'C'}$, and $l_3 = \overline{AC} = \overline{A'C} = \overline{AC'} = \overline{A'C'}$ (Fig. 1). Changes in the distances between parallel struts, $\Delta s_\alpha \equiv s_\alpha - s_0$ ($\alpha = x, y, z$), are referred as extensions. Relationships between distances $s_x$, $s_y$, and $s_z$ and cable lengths $l_1$, $l_2$, and $l_3$ are derived from model geometry, as described in the Appendix. The following relationships are obtained

$$l_1 = 0.5\sqrt{s_x^2 + s_y^2 - 2s_y + 2}, \qquad (1)$$

$$l_2 = 0.5\sqrt{s_y^2 + s_z^2 - 2s_z + 2}, \qquad (2)$$

$$l_3 = 0.5\sqrt{s_z^2 + s_x^2 - 2s_x + 2}. \qquad (3)$$

<center>INTERCONNECTEDNESS</center>

Two cases of interconnectedness are considered. One, where cables and struts are connected by frictionless pin joints at their junctions ("pinned structure"). Consequences of this assumption are: (i) the tension force in each cable segment depends on its length, and (ii) forces acting at each end of a strut or a cable reduce to a single force (tension for cables and compression for struts) and no couples. In the other case the cables run through frictionless loops at the junctions ("looped structure") and thus, they can slide relative to the struts. Consequences of this assumption are: (i) the tension force in the cables depends on the overall cable length, not the length of

an individual segment, and (ii) loops joints transmit only tension and compression forces to cables and struts, respectively, no couples. At the molecular level, the pinned structure could correspond to the case where different CSK filaments are cross-linked or physically bound to one another through intermolecular binding interactions (e.g., microtubules and intermediate filaments through kinesin). In contrast, the looped structure could correspond to the case when those filaments are not cross-linked and can slide relative to each other (e.g., intermediate filaments across actin stress fibers).

<center>EQUILIBRIUM EQUATIONS</center>

*Pinned structure*

From the principle of virtual work it follows that the work of stretching force $T$ during an incremental axial extension of the structure ($\delta s_x$) is equal to the work of tensile forces in the cables ($F_1$, $F_2$, and $F_3$) during corresponding changes of cable lengths ($\delta l_1$, $\delta l_2$, and $\delta l_3$).

$$T\,\delta s_x = 8 \sum_{i=1}^{3} F_i\,\delta l_i. \qquad (4)$$

By substituting eqns (1–3) into eqn (4), the following relationships are obtained

$$T = 2\left(F_1 \frac{s_x}{l_1} + F_3 \frac{s_x - 1}{l_3}\right) \qquad (5)$$

and

$$\text{(a)} \ \ F_1 \frac{1 - s_y}{l_1} = F_2 \frac{s_y}{l_2} \quad \text{and} \quad \text{(b)} \ \ F_2 \frac{1 - s_z}{l_2} = F_3 \frac{s_z}{l_3}. \qquad (6)$$

Equation (5) describes the balance of forces at the joints $A$ and $A'$ along the $Ox$-axis (Fig. 1). Equation (6a) describes the balance of forces at the joints $B$ and $B'$ along the $Oy$-axis and eqn (6b) describes the balance of forces at joints $C$ and $C'$ along the $Oz$-axis (Fig. 1). The balance of forces at the joints in all other directions are satisfied by the symmetry of model geometry.

*Looped structure*

In this case, forces in each cable are equal throughout deformation ($F_1 = F_2 = F_3 \equiv F$) and depend on the overall cable length $L = 8(l_1 + l_2 + l_3)$. Taking these into account, it follows from eqns (5) and (6) that

$$T = 2F\left(\frac{s_x}{l_1} + \frac{s_x - 1}{l_3}\right) \qquad (7)$$

and

$$\text{(a)} \quad \frac{1 - s_y}{l_1} = \frac{s_y}{l_2} \quad \text{and} \quad \text{(b)} \quad \frac{1 - s_z}{l_2} = \frac{s_z}{l_3}. \qquad (8)$$

Equations (7) and (8) represent balance of forces at the joints as described above.

### CABLE ELASTICITY

In this simple starting case, it is assumed that the cables are linearly elastic (i.e., Hookean) and carry only tensile forces. Hence, their force vs. length relationships are given as following

$$F_i = \begin{cases} k(l_i - l_R) & \text{if } l_i > l_R \\ 0 & \text{if } l_i \leqslant l_R \end{cases} \quad (i = 1, 2, 3) \qquad (9)$$

for the pinned structure, and

$$F = \begin{cases} K(L - L_R) & \text{if } L > L_R \\ 0 & \text{if } L \leqslant L_R \end{cases} \qquad (10)$$

for the looped structure. Here $k$ and $K$ denote cable stiffnesses, $l_R$ is the resting (unstressed) length of the cable segment, $l_R \leqslant l_0$, and $L_R = 24l_R$ is the overall resting length of the cable. Since the cable length $l_0 = \sqrt{0.375}$ is well defined, it was used as the reference length in calculating cable strains instead of the resting length $l_R$, which can take any value between 0 and $l_0 (0 < l_R \leqslant l_0)$.

Stretching force vs. axial extension ($T$ vs. $\Delta s_x$) relationships for the model are obtained as following. For a given cable stiffness, and a given initial cable strain $\xi \equiv 1 - l_R/l_0 (0 \leqslant \xi \leqslant 1)$, lateral distances between struts, $s_y$ and $s_z$, are computed from eqns (6a) and (6b) (pinned) and eqns (8a) and (8b) (looped) for a series of values of axial distances, $s_x$. Computed values are used to obtain stretching force $T$ vs. axial extension $\Delta s_x$ relationships from eqn (5) (pinned) and eqn (7) (looped). Structure stiffness is obtained as the ration $E \equiv T/\Delta s_x$. Note that the units of stiffness $E$ are in spring equivalents, i.e., force per unit length. Computations were done numerically, using Mathematica software.

### Results

We began our quantitative analysis of the architectural basis of cell shape stability by varying prestress in the pinned six-strut tensegrity structure. This was accomplished by numerically varying the initial cable strain $\xi$, at a given cable stiffness $k$. Results were obtained for the unit cable stiffness, $k = 1$. The stretching force $T$ increased with increasing axial extension $\Delta s_x$ and, in general, this
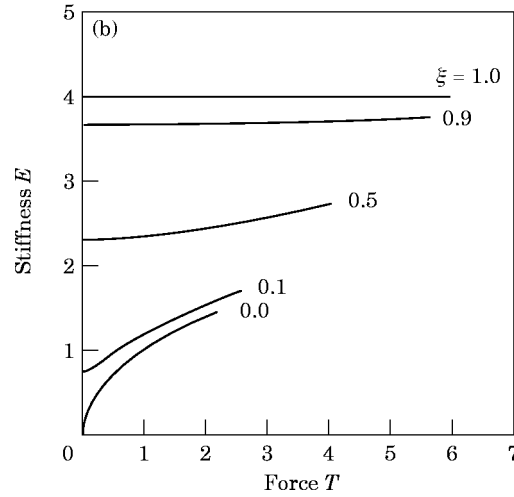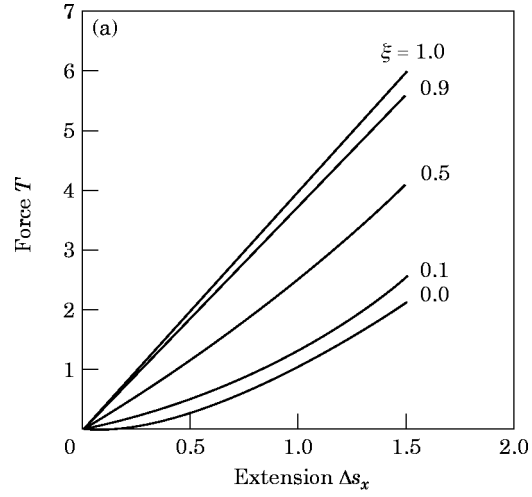


FIG. 2. (a) Stretching force $T$ vs. axial extension $\Delta s_x$ relationship and (b) structural stiffness $E$ vs. stretching force $T$ relationships for the pinned model, for different initial cable strains $\xi$, i.e., different prestresses. Plots were obtained for $\xi$ of 0.0, 0.1, 0.5, 0.9 and 1.0, $k = 1$, and $s_x$ ranging between 0.5 and 2.0. Force is given in units of force, extension in units of length, and stiffness in units of force/length.

dependence was nonlinear [Fig. 2(a)]. This nonlinearity, however, decreased with increasing prestress (i.e., increasing $\xi$) and became linear when the prestress was maximal (i.e., $\xi = 1$). In other words, structural stiffness $E$ increased with increasing stretching force $T$ (stiffening response) [Fig. 2(b)]. This indicates that the resistance of the structure to shape distortion increases with increasing stretching force. The magnitude of the stiffening response decreased with increasing prestress [i.e., the dependence of structural stiffness $E$ on stretching force $T$ decreased with increasing $\xi$; Fig. 2(b)].

The lateral extension $\Delta s_y$ increased [Fig. 3(a)] whereas the lateral extension $\Delta s_z$ first increased and
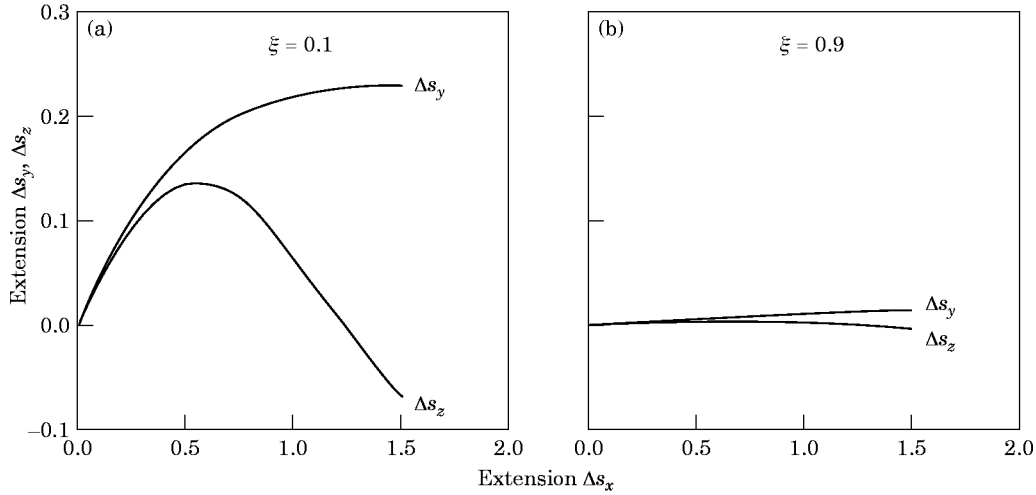
FIG. 3. Lateral extensions $\Delta s_y$ and $\Delta s_z$ vs. axial extension $\Delta s_x$ for the pinned model, for prestresses corresponding to initial cable strains (a) $\xi = 0.1$ and (b) $\xi = 0.9$. Relationships calculated for other values of $\xi$ exhibited qualitatively similar features. Plots were obtained for unit cable stiffness $k = 1$, and $s_x$ ranging between 0.5 and 2.0. Extensions are given in units of length.

then decreased with increasing axial extension $\Delta s_x$ [Fig. 3(b)]. Furthermore, with increasing prestress (i.e., increasing $\xi$), these dependencies diminished such that in the limit where the prestress approached maximum, lateral extensions vanished (i.e., $\Delta s_y, \Delta s_z \to 0$ as $\xi \to 1$). The asymmetry in the dependences of lateral extension $\Delta s_y$ and $\Delta s_z$ on axial extension $\Delta s_x$ implies that the model is not isotropic.

Fractional changes in cable lengths (cable strains) $\Delta l_i/l_0 \equiv (l_i - l_0)/l_0 (i = 1, 2, 3)$ were much smaller than the fractional change of the structure length in the uniaxial direction (uniaxial strain) $\Delta s_x/s_0$ (Fig. 4). In other words, as the entire structure stretches uniaxially, it extends to a much greater degree than its individual cables elongate.

For the looped structure, in order to have the same prestress at a given initial cable strain $\xi$ as in the pinned case, it is assumed that the overall cable stiffness $K = k/24$. Results were obtained for the cable stiffness $K = 1/24$ and for the same values of the initial cable strain $\xi$ and the axial distance $s_x$ as in the pinned case. Stretching force $T$ increased nonlinearly with increasing axial extension $\Delta s_x$ [Fig. 5(a)]. Unlike the pinned structure, structural stiffness $E$ exhibited a "softening" effect at higher values of prestress (i.e., higher $\xi$); stiffness $E$ decreased after an initial increase in response to increasing stretching force $T$ [Fig. 5(b)]. However, for smaller values of prestress (i.e., smaller $\xi$), the model predicts a stiffening effect [Fig. 5(b)]. In comparison with the pinned structure, the looped
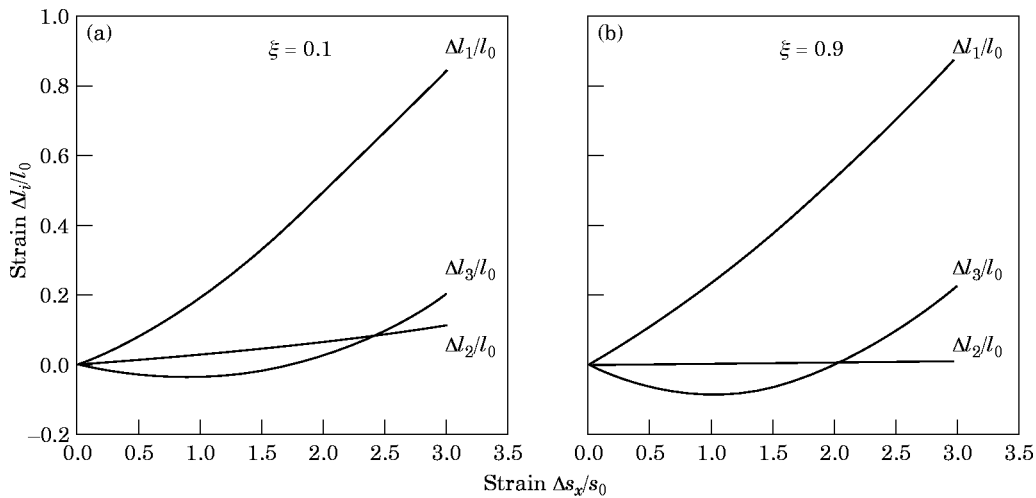


FIG. 4. Cable strain $\Delta l_i/l_0$ ($i = 1, 2, 3$) vs. uniaxial strain of the structure $\Delta s_x/s_0$ for the pinned model, for prestresses corresponding to initial cable strains (a) $\xi = 0.9$ and (b) $\xi = 0.9$. Relationships calculated for other values of $\xi$ exhibited qualitatively similar features. Plots were obtained for unit cable stiffness $k = 1$, and $s_x$ ranging between 0.5 and 2.0.
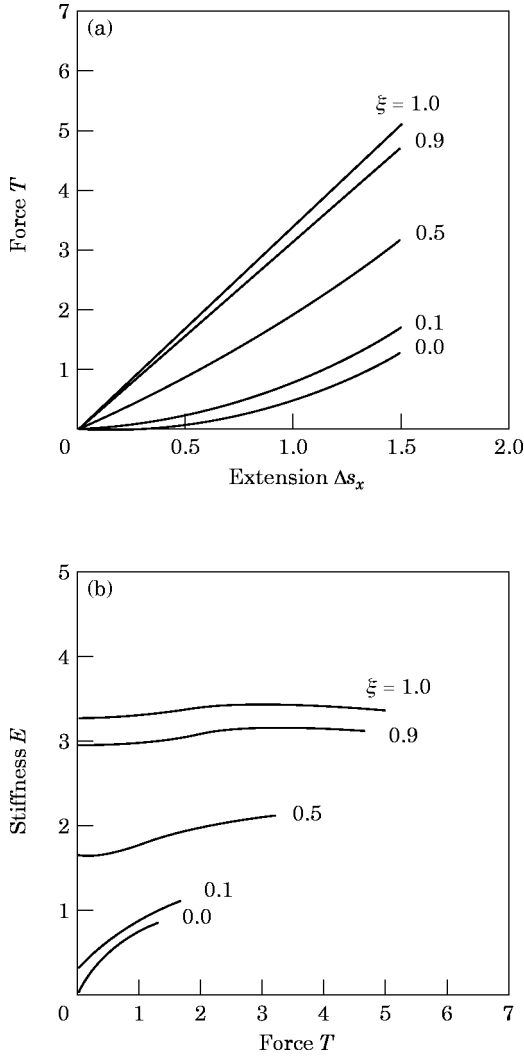
FIG. 5. (a) Stretching force $T$ vs. axial extension $\Delta s_x$ relationship and (b) structural stiffness $E$ vs. stretching force $T$ relationships for the looped model, for different initial cable strains $\xi$, i.e., different prestresses. Force is given in units of force, extension in units of length, and stiffness in units of force/length.

structure is more compliant at a given prestress [Figs 2(b) vs. 5(b)].

For the cable stiffness $K = 1/24$ and for the same values of the initial cable strain $\xi$ and the axial distance $s_x$ as in the pinned case, lateral extension $\Delta s_y$ decreased, whereas lateral extension $\Delta s_z$ first decreased and then increased with increasing axial extension $\Delta s_x$ (Fig. 6). These relationships are opposite to those in the pinned structure [Figs 3(a) and 3(b)] and are independent of prestress (i.e., independent of $\xi$). Again, the asymmetry in the dependences of lateral extensions $\Delta s_y$ and $\Delta s_z$ on the axial extension $\Delta s_x$ implies that the model is not isotropic. In addition, when stretched uniaxially, the looped structure extends much more than the cable
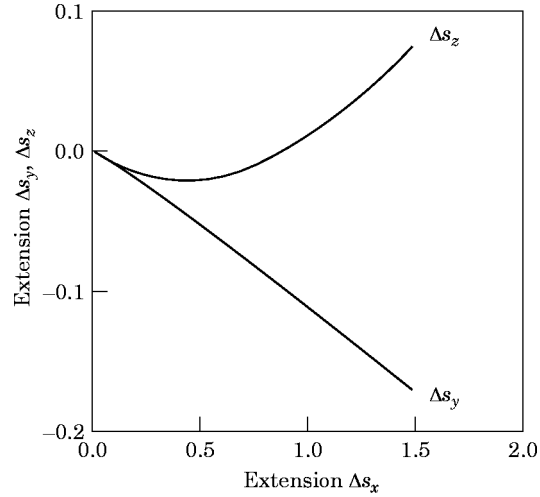


FIG. 6. Lateral extensions $\Delta s_y$ and $\Delta s_z$ vs. axial extension $\Delta s_x$ for the looped model, for all prestresses. Displacements are given in units of length.

elongates, and this effect is independent of prestress (i.e., independent of $\xi$; Fig. 7).

Schematic depictions of structural rearrangements during uniaxial stretching is shown in Fig. 8(a), for the pinned structure, and Fig. 8(b), for the looped structure.

## Discussion

### MECHANISTIC CONSIDERATIONS

The simple architecture of the six-strut tensegrity structure and the deformation it undergoes during uniaxial stretching do not directly correspond to that of the CSK lattice of living cells or the deformation that the CSK undergoes when mechanically stressed. Nevertheless, these simplistic structures have been shown to qualitatively mimic many properties
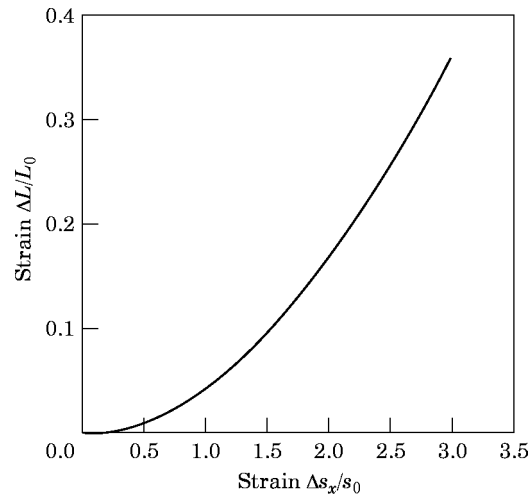


FIG. 7. Overall cable strain $\Delta L/L_0$ vs. uniaxial strain of the structure $\Delta s_x/s_0$ for the looped model, for all prestresses.
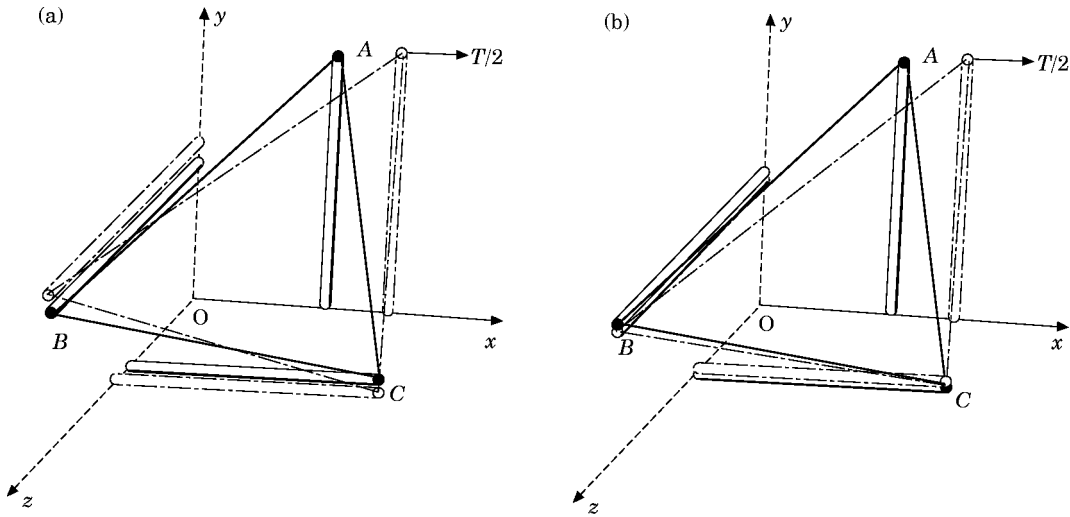
FIG. 8. Structural rearrangements of the pinned (a) and looped (b) six-strut tensegrity structures during the initial phase of uniaxial stretching (i.e., $0 < \Delta s_z < 0.5$). Only the portion of the structure from Fig. 1 inside the first quadrant of the $Oxyz$ coordinate system, including stretching force $T/2$ at point $A$, are shown. The reference configuration is drawn by solid lines and the deformed configuration is drawn by interrupted lines. During the initial phase of stretching of the pinned structure (a), the distances between the pairs of parallel struts increase (i.e., $\Delta s_x > \Delta s_y > \Delta s_z > 0$, Fig. 3) causing, the triangle $ABC$, formed by the cables, to rotate and to change its shape due to change of cable lengths. Thus, stretching of the structure is partly accounted for by rotation of the triangle and partly by cable elongations. In the looped structure (b), however, as the distance between the pulled struts increases (i.e., $\Delta s_x > 0$), the lateral distances decrease initially (i.e., $\Delta s_y < \Delta s_z < 0$, Fig. 6). Thus, the triangle $ABC$ undergoes a little rotation and a considerable shape distortion. Nevertheless, the perimeter of the triangle (i.e., the overall cable length) changes little. The above description of structural rearrangements of the pinned and looped structures explains why when stretched, those structures extend more than the cables elongate.

expressed in living cells (Ingber & Jamieson, 1985; Ingber, 1993a; Ingber *et al.*, 1994). Thus, there is reason to suppose that they may share essential principles of design and a common basis of mechanical stability.

One of the most important results of this study is that the predicted stretching force vs. axial extension ($T$ vs. $\Delta s_x$) relationships of the structure were nonlinear [Figs 2(a) and 5(a)], even though the force vs. extension relationship of the cables was linear [eqns (9) and (10)]. This indicates that mechanical properties of individual structural elements are not the sole determinants of mechanical properties of the integrated structure during its shape distortion. Instead, prestress and architectural features of the structure were found to contribute importantly to its mechanical properties, a finding consistent with results obtained in studies with living cells (Wang *et al.*, 1993). This point can be seen by rewriting eqn (5) as follows

$$T = (k\xi) \times \left[ \left( \frac{1 + \Delta l_1/\xi l_0}{1 + \Delta l_1/l_0} - \frac{1 + \Delta l_3/\xi l_0}{1 + \Delta l_3/l_0} \right) \right.$$
$$\left. + 2 \left( \frac{1 + \Delta l_1/\xi l_0}{1 + \Delta l_1/l_0} + \frac{1 + \Delta l_3/\xi l_0}{1 + \Delta l_3/l_0} \right) \Delta s_x \right]. \quad (11)$$

There are two distinct terms on the r.h.s. of eqn (11).

The term $k\xi$ equals prestress divided by the reference cable length $l_0$. The term in the angular bracket represents the contribution of the structure's architecture (i.e., the geometry of the structure and the manner in which structural elements are interconnected). The prestress determines the initial structural stiffness whereas the architecture determines how the structural stiffness changes during deformation. The only parameter that is common in both terms is the initial cable strain $\xi$. Thus, the degree to which the cables are initially extended contributes to both initial stiffness and change of stiffness during deformation. On the other hand, the cable stiffness $k$ appears only to influence the prestress. Thus, the cable stiffness $k$ only affects the initial stiffness of the entire structure; it does not contribute to the change in stiffness the structure exhibits during deformation. The reason for the latter is that cable elasticity is defined in terms of a single elastic coefficient, $k$ [eqn (9)].

According to the above, it appears that the contribution of the initial cable strain $\xi$ to the structural stiffness $E$ is both through prestress ($k\xi$) and through architecture of the structure whereas the contribution of the cable stiffness $k$ to the structural stiffness $E$ is only through prestress. To illustrate this, we consider the following cases.

In the absence of prestress (i.e., $\xi = 0$) the structure has not initial (i.e., no intrinsic) stiffness (i.e., $E = 0$

when $\Delta s_x = 0$) [Fig. 2(b)]. The structure is very deformable as indicated by lateral extensions $\Delta s_y$ and $\Delta s_z$ which are larger than in any case of a non-zero prestress.

If the prestress were maximal (i.e., $\xi = 1$ for a given $k$), then the structural stiffness would be constant throughout deformation ($E = 4k$ for all $\Delta s_x$) [Fig. 2(b)]. The structure is also not easily deformed as indicated by zero lateral extensions $\Delta s_y$ and $\Delta s_z$.

Note that $\xi = 0$ and $\xi = 1$ define the lower and the upper bounds of prestress. It is unlikely that the prestress in the CSK of living cells would correspond to either one of these limits, but more likely would fall between these limits.

If the prestress is varied isometrically, i.e., if the initial cable strain $\xi$ is fixed and cable stiffness $k$ is varied, the initial structural stiffness will vary proportionately, but the manner in which the stiffness of the entire structure changes during stretching will not. In other words, graphs of structural stiffness vs. stretching force would be mutually parallel with higher stiffnesses corresponding to higher prestress (i.e., higher $k\xi$). This type of response to isometric changes in prestress occurs, for example, in airway smooth muscle cells that are stimulated by contractile agonists (Hubmayr *et al.*, 1995).

This analysis also revealed that at a given prestress the looped structure is more compliant than the pinned one [Figs 2(b) vs. 5(b)]. The reason for this increased deformability is that when looped connections are utilized, there are more unconstrained internal degrees of freedom of motion due to sliding of the cables through the frictionless loops. Thus, under a given stretching force $T$, the looped structure undergoes larger deformation than the corresponding pinned structure and consequently, it is more compliant. Another distinct feature of the looped structure is that during stretching it undergoes the same shape distortion regardless of the prestress (Fig. 6). This behavior is due to the fact that the equilibrium requirements at the joints $B$ and $B'$ [eqn (8a)] and joints $C$ and $C'$ [eqn (8b)] are independent of the prestress (i.e., independent of $\xi$).

### ENERGETIC CONSIDERATIONS

An explanation based on energetics for why the six-strut tensegrity structure has no intrinsic stiffness unless prestressed is rooted in the fact that at the reference state the total cable length $L$ (and hence elastic energy stored) attains a minimum (Kenner, 1976). This can be easily seen in the looped structure and therefore, it is considered first. For small axial extensions, structural stiffness equals the initial slope

of the force vs. extension relationship (i.e., $E \to dT/ds_x$ as $\Delta s_x \to 0$). Thus, it follows from eqn (7) that

$$E_0 = \frac{dT}{ds_x}\Big|_0 = \left(\frac{dF}{ds_x}\frac{\partial L}{\partial s_x}\right)\Big|_0 + F_0 \frac{d}{ds_x}\left(\frac{\partial L}{\partial s_x}\right)\Big|_0, \quad (12)$$

where subscript 0 denotes the function evaluated at the reference (initial) state. Since the total cable length $L$ attains minimum at the reference state, $\partial L/\partial s_x|_0 = 0$ and hence the first term on the r.h.s. of eqn (12) vanishes. Since in the absence of prestress the cables carry no initial force (i.e., $F_0 = 0$), the second term on the r.h.s. of eqn (12) vanishes and hence, the initial structural stiffness $E_0 = 0$. Thus, prestress is necessary for the structure's intrinsic ability to resist shape distortion (i.e., $E_0 > 0$).

The pinned case is considered next. It follows from eqn (5) that

$$E_0 = \frac{dT}{ds_x}\Big|_0 = 8 \sum_{i=1}^{3}\left[\frac{dF_i}{ds_x}\frac{\partial l_i}{\partial s_x} + F_i \frac{d}{ds_x}\left(\frac{\partial l_i}{\partial s_x}\right)\right]\Big|_0$$

$$= 8 \sum_{i=1}^{3}\left[\frac{dF_i}{dl_i}\frac{dl_i}{ds_x}\frac{\partial l_i}{\partial s_x} + F_i \frac{d}{ds_x}\left(\frac{\partial l_i}{\partial s_x}\right)\right]\Big|_0. \quad (13)$$

By differentiating eqns (1–3) and (6) with respect to $s_x$, it is obtained that $dl_i/ds_x|_0 = 0$ ($i = 1, 2, 3$) when the initial cable strain $\xi = 0$. Thus, the first term on the r.h.s. of eqn (13) vanishes. Since in the absence of prestress (i.e., $\xi = 0$) the cables carry no initial forces (i.e., $F_i|_0 = 0$, $i = 1, 2, 3$), the second term on the r.h.s. of eqn (13) also vanishes and hence, the initial structural stiffness $E_0 = 0$. Thus, as in the case of the looped structure, prestress is required for the structure's intrinsic ability to resist shape distortion (i.e., $E_0 > 0$).

In summary, the fact that the total cable length (and hence elastic energy) attains a minimum at the reference state implies that the six-strut tensegrity structure is stable and does not collapse in the absence of prestress. However, prestress provides the initial stiffness $E_0$ to the structure whereas the absence of prestress causes the structure to lack intrinsic ability to resist shape distortion.

### PHENOMENOLOGICAL CONSIDERATIONS

Instructive parallels are evident between the behavior of tensegrity structures and observations in living cells. First, the tensegrity structure exhibits structural stiffness $E$ that increases with increasing level of prestress, for example, due to increased initial strain $\xi$ in the cables [Figs 2(b) and 5(b)]. This result is consistent with the observation that CSK stiffness measured in living endothelial cells increases with

increased cell spreading (Wang & Ingber, 1994) which is, in turn, mediated by the cell extension and the CSK reorganization (Mooney *et al*., 1995). Thus, it is not unreasonable to postulate higher levels of prestress in more highly spread cells, although this remains to be demonstrated experimentally. Second, the tensegrity structure exhibits initial stiffness (stiffness at the reference state) that increases with increasing prestress [Figs 2(b) and 5(b)]. Interestingly, the initial CSK stiffness (i.e., the value extrapolated for CSK stiffness at zero applied stress) in spread endothelial cells has been shown to be higher than that in round cells (Wang & Ingber, 1994), a finding consistent with the possibility that the initial cell stiffness is provided by the prestress in the CSK. Third, the pinned tensegrity structure exhibits stiffness greater than that of the looped structure [Figs 2(b) vs. 5(b)]. This result is consistent with the observation that cross-linking in isolated actin filament networks increases their ability to resist shape distortion (Wachsstock *et al*., 1993) and with the finding that CSK stiffness increases when ATP is depleted and actomyosin cross-bridges are fixed (Wang & Ingber, 1994). Fourth, the tensegrity structure undergoes larger fractional changes of length than its cables when it stretches uniaxially (Figs 5 and 7). Living cells, such as neurites can similarly elongate when mechanically stressed (Dennerll *et al*., 1988) even though individual actin filaments and microtubules are not very extensible (Gittes *et al*., 1993). Finally, the tensegrity structure exhibits stiffening. Although it is not linear over the entire range of observed prestresses (i.e., for $0 \leqslant \xi \leqslant 1$), the stiffening response is close to linear for some prestresses within this range [Figs 2(b) and 5(b)]. This specialized form of stiffening behavior is exhibited by living endothelial cells (Wang *et al*., 1993; Wang & Ingber, 1994) as well as many biological tissues (*cf*. Fung, 1981; Mow *et al*., 1992). Thus, our results support the concept that CSK architecture and the prestress rather than the mechanical properties of its individual filaments, are the primary determinants of cell deformability.

On the other hand, some of the responses of the simple tensegrity structure to uniaxial extension that we observed in the present study do not correspond directly with observations in cells. For example, the structure exhibited a stiffening response that decreased with increasing prestress [Figs 2(b) and 5(b)]. In contrast, data obtained in living endothelial cells (Wang & Ingber, 1994) indicate that the stiffening response increases with increasing cell spreading (i.e., increasing prestress). There are many possible reasons for this discrepancy. First, in the structure treated in this report the reference configuration was always

spherical (round) and the interconnectedness did not change when the prestress was altered. This is not likely the case in living cells; as the cell spreads, CSK architecture transforms from a round to a flat configuration. Moreover, cell spreading may cause changes in prestress that are not entirely related to the extent of spreading but also reflect alterations in interconnectedness or density of the CSK (e.g., altered CSK polymerization) or to biochemical changes in the cell (e.g., calcium influx, changes in ATP levels, protein phosphorylation, etc). Second, the tensegrity structure underwent lateral expansions when it was stretched uniaxially (lateral extension $\Delta s_y$ and/or $\Delta s_z$ increase with increasing axial extension $\Delta s_x$ over a portion or over the entire range of $\Delta s_x$; Figs 3 and 6). This result is the opposite from that exhibited by common materials, including tissues and cells, which undergo lateral contraction when stretched uniaxially. Third, for simplicity in this first attempt at quantitatively modeling the CSK, cables were assumed to be linear elastic (i.e., Hookean) and the struts to be rigid. In contrast, CSK filaments are known to exhibit nonlinear and viscoelastic behavior (Janmey *et al*., 1991; Wachsstock *et al*., 1993). Finally, the model experiences both shape and volumetric deformation during uniaxial stretching (as employed in this study) whereas cells exposed to shear stresses only experience isovolumetric shape deformation (Wang *et al*., 1993; Wang & Ingber, 1994).

The parallel drawn between mechanical behaviors of the pinned vs. looped structures on one hand, and of cross-linked actin networks vs. uncross-linked actin gels (Wachsstock *et al*., 1993) on the other, should also be taken with reservation. One reason is that the model depicts the effect of interconnectedness between two types of structural elements, cables and struts, whereas the published data depict the effect of cross-linking between filaments of a single biopolymer, actin. Another reason is that those data were collected in isolated actin networks, in the absence of prestress. Importantly, these actin gels also do not exhibit linear stiffening behavior (Janmey *et al*., 1991; Wang *et al*., 1993).

In this study we only considered the possible contributions of static tensegrity CSK mechanism to the observable mechanical behavior of living cells exposed to shear stresses. The contributions of cross-link dynamics was not considered. Cross-link dynamics by itself cannot explain linear stiffening. For example, we have shown previously that membrane permeabilized CSK preparations that probably do not undergo significant CSK remodeling still exhibits linear stiffening behavior, although other CSK behaviors (e.g., stiffness, permanent defor-

mation, apparent viscosity) differ significantly (Wang & Ingber, 1994). Furthermore, if dynamic changes in the CSK (e.g., polymerization, geometrical rearrangements, and cross-linking) are stress sensitive (as suggested by the works of Hill & Kirschner, 1981; Dennerll et al., 1988; and Ingber, 1993a), then local dynamic remodeling of the CSK would occur in response to local static stress so as to minimize those stresses. However, at any instant of time, those stresses could be stabilized via tensegrity architecture.

## Conclusions

Despite these reservations, this analysis reveals the quantitative basis of several phenomena that tensegrity architecture expresses. Many of the features are also expressed in endothelial cells and other eukaryotic cells as they resist shape distortion. This is an important observation since it has been customary to view cellular mechanics in terms of continuum mechanics (cf. Elson, 1988; Evans & Yeung, 1989; Fung & Liu, 1993). By considering the discrete nature of the CSK it is possible to obtain forces and deformations that mediate cell shape distortion starting from the first principles of mechanics (e.g., from equilibrium of the adjacent structural elements) as we did in this analysis. The overwhelming weight of morphological evidence indicates that the complex lattice of CSK microfilaments, microtubules, and intermediate filaments (Amos & Amos, 1991; Ingber, 1993a) stretches through the cytoplasm from the cell surface to the nucleus (Fey et al., 1984). Furthermore, the shape stability of many cells has been shown to depend on a balance between tension generated in contractile microfilaments and resisted by internal microtubules (Dennerll et al., 1988; Danowski, 1989; Kolodney & Wysolmerski, 1992; Ingber, 1993a; Heidemann & Buxbaum, 1994). Thus, tensegrity architecture is not an unreasonable starting point for modeling the living cell CSK in adherent cells. Nevertheless, the six-strut tensegrity model must be regarded only as a crude representation of the mechanics of the CSK. Even so, our analysis identified prestress and architecture of the CSK as key features that might underlie a cell's ability to regulate its shape.

## REFERENCES

AMOS, L. A. & AMOS, W. B. (1991). *Molecules of the Cytoskeleton*. New York: Guilford Press.

DANOWSKI, B. A. (1989). Fibroblast contractility and actin organization are stimulated by microtubule inhibitors. *J. Cell Sci*. **93**, 255–266.

DAVIES, P. F. & TRIPATHI, S. C. (1993). Mechanical stress mechanisms and the cell: and endothelial paradigm. *Circ. Res*. **72**, 239–245.

DENNERLL, T. J., JOSHI, H. C., STEEL, V. L., BUXBAUM, R. E. & HEIDEMANN, S. R. (1988). Tension and compression in the cytoskeleton of PC-12 neurites: quantitative measurements. *J. Cell Biol*. **107**, 565–674.

ELSON, E. L. (1988). Cellular mechanics as an indicator of cytoskeletal structure and function. *Ann. Rev. Biophys. Biophys. Chem*. **17**, 397–430.

EVANS, E. & YEUNG, A. (1989). Apparent viscosity and cortical tension of blood granulocytes determined by micropipet aspiration. *Biophys. J*. **56**, 151–160.

FEY, E. G., WANG, K. M. & PENMAN, S. (1984). Epithelial cytoskeletal framework and nuclear matrix-intermediate filament scaffold: three dimensional organization and protein composition. *J. Cell Biol*. **98**, 1973–1984.

FRISÉN, M., MÄGI, M., SONNERUP, I. & VIIDIK, A. (1969). Rheological analysis of soft collagenous tissue—I. *J. Biomech*. **2**, 13–20.

FULLER, B. (1961). Tensegrity. *Portfolio Artnews Annual*. **4**, 112–127.

FUNG, Y. C. (1981). *Biomechanics—Mechanical Properties of Living Tissues*. New York: Springer–Verlag.

FUNG, Y. C. & LIU, S. Q. (1993). Elementary mechanics of the endothelium of blood vessels. *ASME J. Biomech. Eng*. **115**, 1–12.

GITTES, F., MICKEY, B., NETTLETON, J. & HOWARD, J. (1993). Flexural rigidity of microtubules and actin filaments measured from thermal fluctuations shape. *J. Cell Biol*. **120**, 923–934.

HARRIS, A. K., WILD, P. & STOPAK, D. (1980). Silcone rubber substrata: a new wrinkle in the study of cell locomotion. *Science*. **208**, 177–180.

HEIDEMANN, S. R. & BUXBAUM, R. E. (1994). Mechanical tension as a regulator of axonal development. *Neuro Toxicology*. **15**, 95–108.

HILL, T. L. & KIRSCHNER, M. W. (1982). Bioenergetics and kinetics of microtubule and actin filament assembly–disassembly. *Int. Rev. Cytol*. **78**, 1–125.

HUBMAYR, R., SHORE, S. FREDBERG, J., PLANUS, E., PANETTIERI, R. & WANG, N. (1995). Cytoskeletal mechanics of human airway smooth muscle cells. (Abstract). *Respir. Critical Care Med*. **151**, A125.

INGBER, D. E. (1991). Integrins as mechanochemical transducers. *Curr. Opin. Cell. Biol*. **3**, 841–848.

INGBER, D. E. (1993a). Cellular tensegrity: defining new rules of biological design that govern the cytoskeleton. *J. Cell Sci*. **104**, 613–627.

INGBER, D. E. (1993b). The riddle of morphogenesis: a question of solution chemistry or molecular cell engineering? *Cell*. **75**, 1249–1252.

INGBER, D. E. & JAMIESON, J. D. (1985). Cells as tensegrity structures: architectural regulation of hystodifferentiation by physical forces transduced over basement membrane. In: *Gene Expression during Normal and Malignant Differentiation* (Andersson, L. C., Gahmberg, C. G. & Ekblom, P., eds) pp. 13–32, London: Academic Press.

INGBER, D. E., DIKE, L., HANSEN, L., KARP, S., LILEY, H., MANIOTIS, A., et al. (1994). Cellular tensegrity: exploring how mechanical changes in the cytoskeleton regulate cell growth, migration, and tissue pattern during morphogenesis. *Int. Rev. Cytol*. **150**, 173–224.

JANMEY, P. A., EUTENEUER, U., TRAUB, P. & SCHLIWA, M. (1991). Viscoelastic properties of vimentin compared with other filamentous biopolymer networks. *J. Cell Biol*. **113**, 155–160.

JOSHI, H. C., CHU, D., BUXBAUM, R. E. & HEIDEMANN, S. R. (1985).

Tension and compression in the cytoskeleton of PC-12 neurites. *J. Cell Biol*. **101,** 697–705.

KENNER, H. (1976). *Geodesic Math and How to Use It*. Berkeley: University of California Press.

KOLODNEY, M. S. & WYSOLMERSKI, R. B. (1992). Isometric contraction by fibroblasts and endothelial cells in tissue culture: a quantitative study. *J. Cell Biol*. **117,** 73–82.

MCMAHON, T. A. (1984). *Muscles, Reflexes, and Locomotion*. Princeton: Princeton University Press.

MOONEY, D., LANGER, R. & INGBER, D. E. (1995). Cytoskeletal filament assembly and the control of cell shape and function by extracellular matrix. *J. Cell Sci*. **108,** 2311–2320.

MOW, V. C., RATCLIFFE, A. & POOLE, A. R. (1992). Cartilage and diarthrodial joints as paradigms for hierarchical materials and structures. *Biomaterials*. **13,** 67–97.

PUGH, A. (1976). *Introduction to Tensegrity*. Berkeley: University of California Press.

SCHIRO, J. A., CHAN, B. M., ROSWIT, W. T., KASSNER, P. D., PENTLAND, A. P., *et al*. (1991). Integrin $\alpha 2\beta 1$ (VLA 2) mediates reorganization and contraction of collagen matrices by human cells. *Cell*. **67,** 403–410.

SCHMIDT, C. E., HORWITZ, A. E., LAUFFENBURGER, D. A. & SHEETZ, M. P. (1993). Integrin-cytolskeletal interactions in migrating fibroblasts are dynamic, symmetric, and regulated. *J. Cell Biol*. **123,** 977–991.

SCOTT-BURDEN, T. (1994). Extracellular matrix: the cellular environment. *NIPS* **9,** 110–115.

STAMENOVIĆ, D. (1991). A model of foam elasticity based upon the laws of Plateau. *J. Colloid Interface Sci*. **145,** 255–259.

WANG, N. & INGBER, D. E. (1994). Control of the cytoskeletal mechanics by extracellular matrix, cell shape, and mechanical tension. *Biophys. J*. **66,** 2181–2189.

WANG, N., BUTLER, J. P. & INGBER, D. E. (1993). Mechanotransduction across the cell surface and through the cytoskeleton. *Science*. **260,** 1124–1127.

WACHSSTOCK, D. H., SCHWARZ, W. H. & POLLARD, T. D. (1993). Affinity of α-actinin for actin determines the structure and mechanical properties of actin filament gels. *Biophys. J*. **65,** 205–214.

# APPENDIX

A derivation of the expression for $l_1$ as a function of $s_x$ and $s_y$, eqn (1), is given below. It is based on the derivation of Kenner (1976).

Figure A1 depicts the portion of the six-strut tensegrity structure from Fig. 1 inside the first quadrant of the coordinate system *Oxyz*; $\overline{AB} = l_1$, $\overline{OA_x} = s_x/2$, $\overline{OB_y} = s_y/2$, $\overline{AA_x} = 1/2$, and $\overline{BB_y} = 1/2$. Thus,

$$l_1 = \sqrt{\overline{AB_y^2} + \overline{BB_y^2}}$$

$$= \sqrt{\overline{OA_x^2} + (\overline{AA_x} - \overline{OB_y})^2 + \overline{BB_y^2}}$$

$$= 0.5\sqrt{s_x^2 + s_y^2 - 2s_y + 2}.$$

The expressions for $l_2$ and $l_3$ given by eqns (2) and (3) can be obtained in a similar manner.



FIG. A1. The portion of the six-strut tensegrity structure (Fig. 1) inside the first quadrant of the *Oxyz* coordinate system.

### Nomenclature

$F_i$ = force in the *i*-th cable of the pined structure ($i = 1, 2, 3$)

$F$ = force in the cable of the looped structure

$k$ = cable stiffness of the pinned structure

$K$ = cable stiffness of the looped structure

$l_i$ = length of the *i*-th cable ($i = 1, 2, 3$)

$l_0 = \sqrt{0.375}$ = reference length of the cables

$l_R$ = resting length of the cables

$\Delta l_i \equiv l_i - l_0$ = elongation of the *i*-th cable ($i = 1, 2, 3$)

$\xi \equiv 1 - l_R/l_0$ = initial cable strain

$L = 8(l_1 + l_2 + l_3)$ = overall cable length

$L_0 = 24 l_0$ = overall reference cable length

$L_R = 24 l_R$ = overall resting cable length

$\Delta L \equiv L - L_0$ = overall cable elongation

$s_\alpha$ = distance between pairs of parallel struts ($\alpha = x, y, z$)

$s_0 = 0.5$ = distance between parallel struts at the reference state

$\Delta s_\alpha \equiv s_\alpha - s_0$ = structural extension ($\alpha = x, y, z$)

$T$ = stretching force

$E \equiv T/\Delta s_x$ = structural stiffness

CSK = cytoskeleton